Radiative cooling of C 7

K. Najafian, M. S. Pettersson, B. Dynefors, H. Shiromaru, J. Matsumoto, H. Tanuma, T. Furukawa, T. Azuma, and K. Hansen

Citation: The Journal of Chemical Physics **140**, 104311 (2014); doi: 10.1063/1.4867499
View online: http://dx.doi.org/10.1063/1.4867499
View Table of Contents: http://scitation.aip.org/content/aip/journal/jcp/140/10?ver=pdfcov
Published by the AIP Publishing

Radiative cooling of C_7^-

K. Najafian,[1] M. S. Pettersson,[1] B. Dynefors,[2] H. Shiromaru,[3] J. Matsumoto,[3] H. Tanuma,[4] T. Furukawa,[4] T. Azuma,[5] and K. Hansen[1]
[1]*Department of Physics, University of Gothenburg, 41296 Gothenburg, Sweden*
[2]*Applied Physics, Chalmers Technical University, Gothenburg, Sweden*
[3]*Department of Chemistry, Tokyo Metropolitan University, 1-1 Minamiosawa, Hachiouji-shi, Tokyo 192-0397, Japan*
[4]*Department of Physics, Tokyo Metropolitan University, 1-1 Minamiosawa, Hachiouji-shi, Tokyo 192-0397, Japan*
[5]*Atomic, Molecular and Optical Physics Laboratory, RIKEN, 2-1 Hirosawa, Wako-shi, Saitama 351-0198, Japan*

(Received 3 December 2013; accepted 21 February 2014; published online 13 March 2014)

The spontaneous and photo-induced neutralization of C_7^- produced in a laser ablation source was measured in an electrostatic storage ring. The measurements provide three independent determinations of the radiative cooling of the ions, based on the short time spontaneous decay and on the integrated amplitude and the shape of the photo-induced neutralization signal. The amplitude of the photo-induced signal was measured between 0.5 ms and 35 ms and found to depend on photon wavelength and ion storage time. All three signals can be reproduced with identical thermal IR radiative cooling rates with oscillator strengths equal to theoretical predictions. In addition, the measurements provide the excitation energy distribution. © *2014 AIP Publishing LLC*. [http://dx.doi.org/10.1063/1.4867499]

INTRODUCTION

Radiative cooling is an important factor for determining the abundance of molecules and clusters in dilute gasses and in particular in the very good vacuum of interplanetary and interstellar space. In this environment, collisional relaxation plays a minor role in the dissipation of excess molecular energy which is predominantly dissipated in unimolecular reactions or as radiation. With the increasing number of carbon-containing molecules and ions discovered in space,[1] the fate of highly excited states of these molecules has gained in importance.

The radiative cooling of a number of fullerenes has already been studied in detail. Experimentally it was found that the cooling is significantly higher than could be explained by pure infrared emission, both for anions and cations.[2–5] The enhanced radiative cooling originates in the surface plasmon resonance, which extends to low energies and quantitatively accounts for the thermal radiation from the fullerenes.[6] For small molecules, on the other hand, both electronic and vibrational radiation can be important. The radiation from C_5^- is exclusively of vibrational origin,[7] whereas C_6^- and the anthracene anion, on the other hand, cool via radiation from a single, thermally excited, low lying electronic excitation.[8,9]

In this work we report on studies of the cooling of C_7^-. The interpretation of the experiments will be accompanied by simulations of the infrared cooling based on previously published IR integrated absorption coefficients. In addition, the time profile of laser enhanced decays will be analyzed in detail.

EXPERIMENTAL PROCEDURE

The experimental setup has been reported previously in Ref. 10 and we will only give a brief summary here. The anions were produced in a laser ablation source with a several ns laser pulse from a frequency doubled Nd:YAG laser, lightly focused and with pulse energy of 1–2 mJ. The target was a rotating graphite disk floated to a high voltage. For reasons of pressure the source operated without any cooling gas and the produced clusters expanded directly from the surface into vacuum. After acceleration to 15 keV the ions were injected into the ring and unwanted masses rejected with a pulsed electric field.[10] This purification phase was completed 0.23 ms after injection. The ions decayed spontaneously for a few ms, with only a weak, long lived tail visible for longer times. The main part of the decay from several ms were either caused by collision with rest gas or absorption of a photon from a tunable OPO (Optical Parametric Oscillator) laser. The rest-gas collision-induced decay was exponential with a time constant exceeding 0.3 s. Figure 1 shows two typical spectra, one with and one without photoinduced decay.

After a storage time that varied from 0.5 ms to 35 ms, the ions were exposed to a nanosecond laser pulse. The neutralization yield was measured time-resolved by detecting the neutral signal at the end of the straight section opposite to the side of the ring where the photon absorption occurs. The time resolution was given by the circulation time in the ring (46 μs). The position of laser excitation and neutrals detection means that the neutralization signal is measured in well defined time intervals of a few μs centered on odd multiples of half the circulation time of

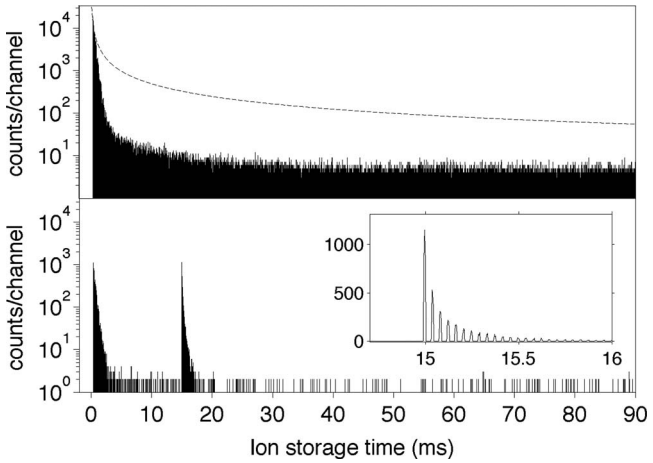

FIG. 1. Top frame: Spontaneous decay of C_7^- as produced in the source. The dotted line is the $1/t$ decay expected in the absence of radiative cooling. Bottom frame: Photo-induced (enhanced) decay for a laser pulse at 15 ms. The measured signal is the neutral clusters count produced in the process $C_7^- \rightarrow C_7 + e^-$. The detector is placed at the end of the straight section on the same side of the ring as the source and opposite to the side of the photo-absorption. The number of ion injections in the bottom frame is an order of magnitude less than the top frame. The inset gives an expanded view on linear scale of the measured decay rate. The peaks correspond to decay within the same circulation period in the ring.

the ion in the ring, $(2n + 1)23\ \mu$s, with n a non-negative integer.

Three different photon energies (wavelengths) were used: 2.695 eV (460 nm), 2.398 eV (517 nm), and 2.101 eV (590 nm). The photo-induced signal, of which an example is shown in the inset in Fig. 1, decreases rapidly, over 10–20 revolutions in the ring. Both the decay and the time integral of this signal will be analyzed below.

The small heat capacity of the clusters allows for a significant experimental simplification. It gives a very high electron emission rate constant, k_e, if more than one photon is absorbed. This is illustrated in Fig. 2 which shows k_e, calculated below, for electron emission vs. energy.

Twice the photon energy of the longest wavelength used are indicated. Even for this very conservative estimate where no excitation energy is present in the ion prior to laser excitation will the absorption of two or more photons give cause

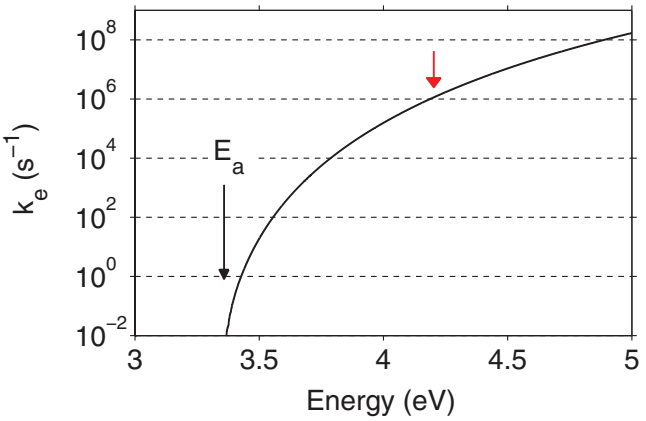

FIG. 2. The theoretical electron emission rate constant vs. internal energy, as given by Eq. (3). The energy of two photons of the longest wavelength used is indicated by the upper arrow.

emission on a time scale significantly below the time the ions take to move from the excitation region to the detection area (23 μs). Ions that absorb more than one photon were therefore not detected in these experiments. It was therefore possible to use a laser power that optimized the magnitude of the detected signal. The fluence dependence was measured for all three photon energies. At low fluence the neutralization yield increased. The increase was sub-linear, possibly because the absorption cross sections for the second photon is larger than for the first. At higher pulse energies the yield flattened out and at the highest pulse energies it decreased with increasing energy. The flat part of the curve was located between 1 and 4 mJ/pulse for the three wavelengths and these energies were used in the experiments. Thus, the signal was independent of fluence to first order and the effects of fluctuations in laser power therefore minimized.

RESULTS

The total data set consists of the spontaneous decay rate shortly after injection into the ring, of the laser enhanced neutralization yield, and of the time dependence of this yield. We will first analyse the magnitude of the enhanced signal after photon absorption as a function of the storage time.

The photo-induced signal is shown in Fig. 3 for all three photon energies used. This signal is the sum of the first five peaks after photon absorption, after background subtraction and a normalization to the width of the ion package and intensity of the source. Very little difference was seen when instead only the first or the first three peaks were included in the signal, and the choice of five peaks was made for reasons of statistics. For the source intensity we use the count rate integrated between 0.3 and 0.5 ms as a proxy. No normalization to the photon flux is required, as explained above. The absolute intensity scales are related to the photon absorption cross sections and the decay dynamics and will not be analyzed here.

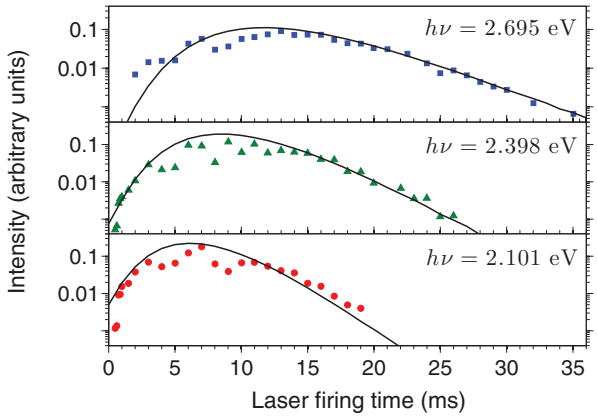

FIG. 3. The laser enhanced signal for the three different photon energies at several laser firing times. Photon wavelengths top to bottom: 460 nm, 517 nm, and 590 nm. The lines are simulations of the signal as modeled including the effect of radiative cooling. The experimental data at different laser firing times were normalized to the pre-laser shot source intensities. The data and the simulations have both been normalized with an arbitrary constant for each photon energy to give similar peak values. Details of the simulations are given in the main text.

The curves all have an increasing part at short times and decrease at long times. The precise shape of the curves vary with the photon energy, where the lower photon energy curves peak closer to injection time. The general behavior of the curves is similar to those for C_5^-[7] and the time dependence for the C_7^- signal can be assigned to radiative cooling with arguments identical to those for C_5^-. Briefly, in the absence of radiative cooling and electronically excited states, the neutralization yield would be a constant. Furthermore, the time dependence is inconsistent with a single long-lived excited electronic state. The fact that the time dependence shifts with wavelength rules out any reasonable simple combination of several excited electronic states. The presence of a single excited state gives a monotonous approach to the long time yield. For each wavelength it requires the decay of at least two electronically excited states to produce yield curves that increase and decrease with time, as observed. For three different wavelengths with their different time dependences the numbers of required states triples to six.

We therefore conclude that the decays are statistical and that the photo-excitation energy is distributed over the vibrational manifold of the ions. This conclusion will be corroborated below when the time dependence of the enhanced signal is analyzed and found to indicate a thermal decay.

Before describing the analysis of the cooling we remark on the difference in the description of cooling of the fullerenes and smaller ions, such as C_7^-. For molecules with sufficiently small heat capacities, the emission of a single IR photon quenches the unimolecular decay. The ratio of the photon emission rate constant k_{ph} and the electron emission rate constant, k_{e} or more generally the unimolecular rate constant, then directly determines the branching between radiative cooling and loss of an electron. For molecules with a sufficiently large heat capacity, such as the fullerenes, the radiation can be considered continuous because the change in the rate constant upon a photon emission is relatively small. For a quantitative estimate we note that continuous cooling requires that the relative change of the rate constant upon photon emission, $h\bar{\nu}d\ln k_{\mathrm{e}}(E)/dE$, is less than a constant which is on the order of unity ($\bar{\nu}$ is the mean emitted photon frequency and E is the excitation energy). The criterion states that the emission of a single photon is not sufficient to quench further decay by electron emission. With an Arrhenius expression for $k_{\mathrm{e}}(E)$ and setting $k_{\mathrm{e}}(E)^{-1} \sim t$ (the measurement time), the criterion for continuous cooling is calculated to $C \gg h\bar{\nu}(\ln(\omega t))^2/\Phi$, where ω is the frequency factor in the Arrhenius approximation of Eq. (3), Φ is the electron affinity (EA), and the heat capacity C is given in units of k_{B}. For $h\bar{\nu} = 0.225$ eV, $\Phi = 3.36$ eV and the typical value $\ln(\omega t) = 25$ see, e.g., Refs. 11 or 12 for values of ω, this gives a right-hand side of 41 k_{B}. Even the somewhat crude nature of this calculation shows that this is above any realistic value for C_7^-, for which the harmonic approximation of the linear configuration gives the canonical heat capacity 16 k_{B}. The effect of the radiative cooling is therefore best described by considering the emission of single photons with relatively high energy.

The cooling was simulated with Monte Carlo (MC) calculations. Two vibrational modes are IR active and they have the quantum energies $h\nu_1 = 0.216$ eV and $h\nu_2 = 0.234$ eV.[13] They emit photons with the photon emission rate constant, similar to the one used in Ref. 7,

$$\begin{aligned} k_{\mathrm{ph}}(E) &= \sigma_1 \frac{8\pi\nu_1^3}{c^2}\frac{1}{\rho(E)}\sum_{n=0}^{\infty} n\rho^{(1)}(E - nh\nu_1) \\ &\quad + \sigma_2 \frac{8\pi\nu_2^3}{c^2}\frac{1}{\rho(E)}\sum_{n=0}^{\infty} n\rho^{(2)}(E - nh\nu_2) \\ &\equiv k_{\mathrm{ph},1}(E) + k_{\mathrm{ph},2}(E), \end{aligned} \tag{1}$$

where ρ is the level density for all vibrational modes and $\rho^{(i)}$ ($i = 1, 2$) are the level densities of the 15 oscillator system where the emitting mode i has been excluded. Vibrational frequencies from Ref. 13 were used and scaled to 95% of the calculated values.[14] The photon absorption cross section σ_i is given by $f_i c \ln(10)/N_{\mathrm{A}}\nu_i$, where $f_1 = 2331$ km/mole and $f_2 = 157$ km/mole are the IR integrated absorption coefficients of each emitting mode. The emitted power per ion is correspondingly

$$P(E) = \hbar\omega_1 k_{\mathrm{ph},1}(E) + \hbar\omega_2 k_{\mathrm{ph},2}(E). \tag{2}$$

The channel that gives rise to a signal in the detector is expected to be electron emission. The contribution from other decay channels can be estimated from comparison of activation energies of the different channels. Electron affinities of small carbon clusters from photo-electron spectroscopy[15] and calculations of dissociation energies of neutral carbon clusters[16] give the dissociation energies of C_7^- for the different neutralization channels. The process $C_7^- \rightarrow C_4^- + C_3$ has the lowest calculated dissociation energy with a value of 5.0 eV, considerably higher than the EA of C_7^- of 3.36 eV. Evaporation of C_3 is also found to be the most likely atomic fragment emitted from small neutral carbon clusters.[17]

The thermionic (electron emission) rate constant is given by the detailed balance expression[11,12]

$$k_{\mathrm{e}}(E) = \int_0^{E-E_{\mathrm{a}}} \frac{2m_e}{\pi^2\hbar^3}\epsilon\sigma_c(\epsilon)\frac{\rho_{C_7}(E - E_{\mathrm{a}} - \epsilon)}{\rho_{C_7^-}(E)}d\epsilon, \tag{3}$$

where m_e is the mass of the electron, ϵ the kinetic energy of the decay channel (essentially the electron kinetic energy), σ_c the kinetic energy dependent capture cross section of the reverse process, the ρ's the level densities of the species given by the subscripts, including their electronic degeneracies, and E_{a} the activation energy which is the electron affinity, $E_{\mathrm{a}} = \Phi = 3.36$ eV.[15] The equation gives the rate constant for the statistical emission of an electron in a process where the excitation and the decay is decoupled such that the decay proceeds independently of the precise method of excitation. It is the electron emission analogue to unimolecular decay.

We have simulated the effect of the radiative cooling on both the spontaneous and the photo-induced decay with Monte Carlo simulations, based on Eqs. (1)–(3). The simulations proceeded by recording a large number of decay chains of clusters emitting both photons and electrons and tracing the energies of the surviving cluster anions with time. For one decay chain, an initial excitation energy is selected from a Gaussian distribution. The precise shape of this distribution was not important, only its mean and width. It was found that the mean 3.15 eV and the standard deviation 0.5 eV gave the

best agreement with the data. The decay time for the photon emission, t_{ph}, was found by generating an exponential distribution with the 1/e lifetime $1/(k_{ph,1} + k_{ph,2})$. The competing electron emission was included by generating an exponentially distributed electron emission time, t_e, using $k_e(E_n)$. If $t_e < t_{ph}$ the cluster decays by electron emission, a neutralization event is registered and the decay chain is stopped. If instead a photon emission occurred, the energy of the emitted photon is chosen according to the relative magnitudes of $k_{ph,1}$ and $k_{ph,2}$. The relevant photon energy is subtracted from the energy and the time and energy stored. The process is repeated until the time exceeds 50 ms. All random numbers were calculated according to the methods given in Ref. 18.

Corresponding to the experimental procedure, the energy distribution of the clusters in such a decay chain was probed from 0 to 50 ms in intervals of 1 ms by adding one laser photon energy E_{las} to the energy of the cluster, E. To match the experiment, three different laser photon energies were used, $E_{las}^{(1,2,3)} = 2.695$ eV, 2.398 eV, 2.101 eV. A count is registered at time t with a probability proportional to $k_e(E + E_{las})$ $\exp(-k_e(E + E_{las}) \cdot 23\ \mu s)$. This corresponds to the probability distribution that an anion emits an electron thermally 23 μs after photo-excitation if it has the energy E prior to excitation, and is the product of the post-absorption rate constant and the survival probability of the excited ions, given by the exponential. The 23 μs in the exponential is the time it takes the ion to move from the photo-excitation region to the detection region.

This detection efficiency curve is approximately Gaussian and centered at $E + E_{las} = 3.89$ eV. It is fairly narrow with a full-width-half-maximum of 0.19 eV, and is normalized to unity at its peak value. It determines whether or not a given anion in the ensemble will be detected. The use of a distribution instead of a single energy, as in Ref. 7, becomes more important as the size of the cluster increases. The procedure was repeated until 5×10^5 decay chains had been sampled for the energy distributions. The required statistics was less for other sampled quantities.

The agreement between the simulated and measured data, shown in Fig. 3 is satisfactory, considering that the only free parameters in the simulations are the mean and the width of the zero time energy distribution, although deviations beyond those caused by varying beam overlap can be seen.

We now turn to the analysis of the shape of the enhancement signal immediately after photon absorption. The data provide good statistics for typically 10 turns in the ring (400–500 μs) after photon absorption. An example of the signal is shown in the inset of Fig. 1. Although the overall amplitude of the signal differs significantly, almost identical time dependences were observed for different laser firing times and different wavelengths. The peaks for each turn were integrated after subtraction of the small background. Averages of these integrated, time-resolved signals are plotted in Fig. 4, normalized such that the count over the ten turns sum to unity. Also the simulated decays are shown, calculated with the parameters given above.

The decay profiles are very similar, although the decays for the long storage time data are noticeably slower. This most likely reflects the shape of the energy distribution, and is reproduced very accurately by the simulations. One must expect a slower decrease of the signal for negative slopes of the energy distribution than for positive because for negative slopes relatively more will decay at a later time, and vice versa for positive slopes (for quantitative details see Ref. 12). The only discrepancy between data and simulations is found for the short time data, where the simulations predict a steeper decrease than observed. The short time enhancements in Fig. 3 were also difficult to fit, but it is not clear if these two problems are related.

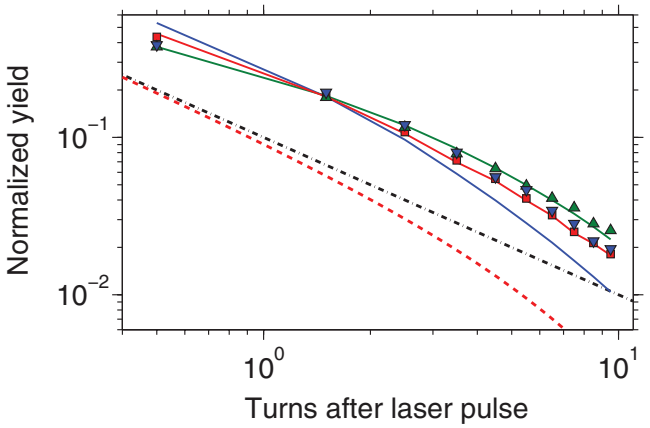

FIG. 4. Decay of the enhanced signal after laser excitation. The figure includes data from the long (up triangles), intermediate (squares), and short laser firing times (down triangles), for all three laser energies. The terms short, intermediate, and long refer to 5, 6–18, and 19–25 ms for 460 nm; 1–3, 4–13, and 14–21 ms for 517 nm, and finally 1–2, 3–10, and 12–15 ms for 590 nm. Each point is an average of 10–30 different spectra. The solid line shows the decay calculated in the MC simulations. The dashed-dotted line is the $1/t$ dependence and the dashed line is the radiatively modified $1/t$ given in Eq. (4), shifted vertically with the same amount as the $1/t$ curve.

The non-exponential decay of the enhanced signal after laser excitation is a strong indication that the decay is thermal. This is corroborated by the nearly identical shapes of the curves for the different photon energies and for different laser firing times.

Next we turn to the shape of the spontaneous decay shortly after injection. As for the decay of the photon induced signal in Fig. 4, it is not exponential. Although closer to a powerlaw decay, it nevertheless also deviates from this. The $1/t$ rate is the expected form when the decay is statistical, there are no competing channels and the clusters are produced with a broad internal energy distribution.[19] With a competing radiative channel the decay rate is modified to a quasi-exponential form.[3] In the first approximation the decay rate can be described with the function

$$I(t) \propto 1/t \rightarrow I(t) \propto \frac{1}{\exp(t/\tau) - 1}, \tag{4}$$

where τ is related to the radiatively emitted power, P, from a cluster with given initial energy E as[2]

$$k_e(E,t) = k_e(E) \exp\left(-\frac{d \ln k_e(E,0)}{dE} Pt\right) \equiv k_e(E,0) \exp(-t/\tau), \tag{5}$$

where $k_e(E)$ is the zero time rate constant given by Eq. (3). The fit of Eq. (4) is shown in Fig. 5. The fit is reasonable at

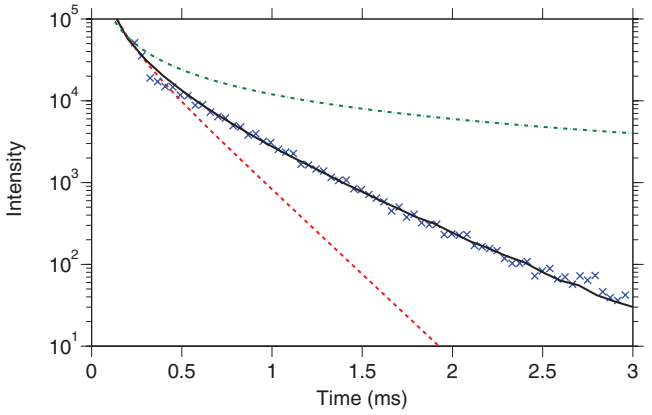

FIG. 5. Spontaneous neutralization yield as a function of time. Crosses: Experimental data. Solid line: Simulation of the spontaneous decay, including radiative cooling. Dashed-dotted line: $1/t$ decay, normalized to the first measured point. Apart from an overall intensity factor, this curve contains no adjustable parameters. Dashed line: Eq. (4) with $\tau = 0.2$ ms, fitted from the short time experimental data.

short times and much poorer at longer times, which is to be expected from the discussion of discrete vs. continuous energy loss. To a sufficient approximation the derivative of the rate constant can be evaluated with an Arrhenius expression for energies corresponding to the rate constant $k_e(E, 0) = 1/\tau$. With a frequency factor of 10^{14} s^{-1}, the precise value of which is not critical, this gives an emitted power at $t = \tau$ of

$$P = \frac{(C-1)\Phi}{\tau(\ln(\omega\tau))^2}, \tag{6}$$

where, as above, C is the canonical heat capacity in units of k_B, and Φ is the activation energy for the process. With Φ equal to the electron affinity 3.36 eV,[15] and the fitted value $\tau = 0.2$ ms the power becomes $P = 425$ eV/s. The combined statistical and systematic uncertainty of this value is probably closer to 100 eV/s than to 10 eV/s.

With the expression for $k_e(E, 0)$ in Eq. (3) one can calculate the average internal energy of the emitting ions at $t = \tau = 0.2$ ms by setting $k_e(E, 0) = 1/\tau$ and solve for E. The value is 3.74 eV, close to the value for E_0 of 3.89 eV. Although τ is an order of magnitude longer than the time that determines E_0, the rapid variation of the rate constant with energy causes these two energies to be very similar, with the energy pertaining to the longer time slightly lower. Combined with the expression for the emitted IR power in Eq. (2), plotted in Fig. 6, it is possible to calculate the expected emitted power. This theoretical emitted power at the energy is equal to 400 eV/s (see Fig. 6). The very good agreement with the value extracted from the fitted τ and the expression for the rate constant alone is probably fortuitous, given the uncertainties in τ due to both experimental uncertainties (the presence of betatron oscillations), to the fact that the fit is performed at times that are not short compared to τ, and to the description of radiation as a continuous process, as discussed above.

The data shown in Fig. 3 have the same general behavior for all three photon energies. A similar phenomenon has been observed for C_5^-,[7] where it was found that the yields could be plotted on the same curve if the times were multiplied with a dimensionless factor, constant for each photon energy. The

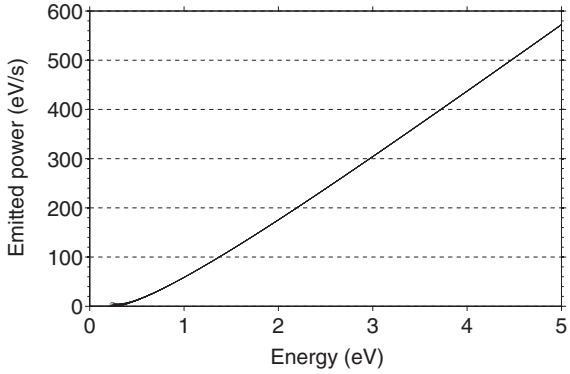

FIG. 6. Calculated radiative cooling power (Eq. (2)) as a function of energy.

scaling is expressed mathematically as

$$I(E_0 - h\nu, t_{las}) = s(E_0 - h\nu)g(s(E_0 - h\nu)t_{las}), \tag{7}$$

where g is a scaling function and s the photon energy dependent scaling factor. The measured yields in Fig. 3 were indeed found, after normalization, to follow such a scaling. If, for simplicity, we assume that all decaying ions have the energy $E_0 \equiv 3.89$ eV (the maximum of the detection efficiency curve), the scale factors s were determined to 0.62 for 460 nm, 0.78 for 517 nm, and 1.08 for 590 nm. This scaling can be used to convert the measured yields over laser firing times into energy distributions for a specific time. With Eq. (7) one converts to a reference time t_{ref},

$$\begin{aligned} I(E_0 - h\nu, t_{las}) &= s(E_0 - h\nu)g\left(s(E_0 - h\nu)\frac{t_{las}}{t_{ref}}t_{ref}\right) \\ &= \frac{s(E_0 - h\nu)}{s(E_0 - h\nu')}I(E_0 - h\nu', t_{ref}), \end{aligned} \tag{8}$$

where $h\nu'$ is defined as (s^{-1} being the inverse function of s)

$$E_0 - h\nu' \equiv s^{-1}\left(s(E_0 - h\nu)\frac{t_{las}}{t_{ref}}\right). \tag{9}$$

From the data the relation between s and $E_0 - h\nu$ is found to be well represented by the empirical formula

$$E_0 - h\nu = 1.7s^{0.69}\,\text{eV}. \tag{10}$$

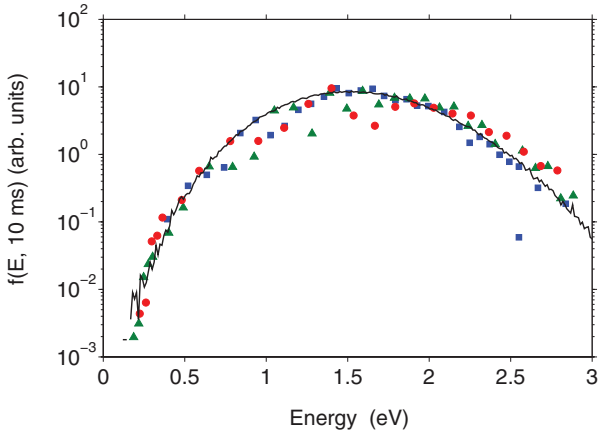

FIG. 7. The energy distribution $f(E)$ at 10 ms, as calculated from the experimental data with Eq. (11). Symbols as in Fig. 3. For the simulation, shown as a line, the energy values were multiplied by 1.2.

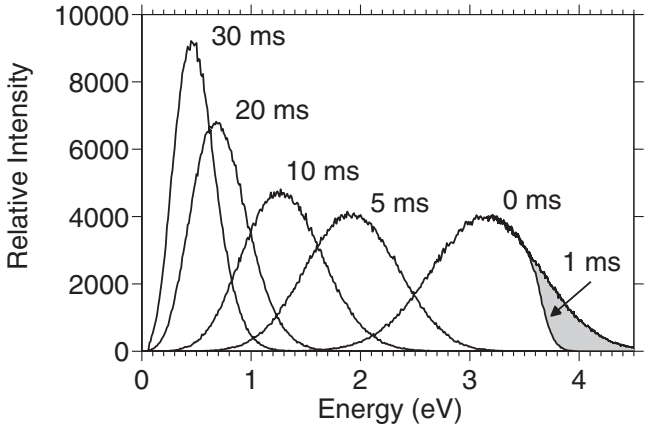

FIG. 8. Energy distributions at $t = 0$, 1, 5, 10, 20, 30 ms from the MC simulations with no photon absorption. Between 0 and 1 ms, the hottest 14% of the ions lose the electron (hatched area). After 1 ms, the energy-integrated intensities are almost identical for all distributions because the bulk part of the distributions are below the electron affinity.

With this, Eq. (8) can be expressed as

$$I(E, t_{\text{ref}}) = \frac{t_{\text{las}}}{t_{\text{ref}}} I(E_0 - h\nu, t_{\text{las}}), \tag{11}$$

where the energy argument is

$$E \equiv E_0 - h\nu' = (E_0 - h\nu)\left(\frac{t_{\text{las}}}{t_{\text{ref}}}\right)^{0.69}. \tag{12}$$

The right-hand side of Eq. (11) is the experimentally observed yields multiplied by a known ratio of two times. Application of Eqs. (11) and (12) with $t_{\text{ref}} = 10$ ms gives the distribution shown in Fig. 7.

The experimental and simulated distributions for 10 ms have similar widths of 0.8 eV (full width half maximum). The experimental distributions have the centroid at 1.5 eV, vs. 1.3 eV for the simulated. We find the agreement satisfactory. Other examples of energy distributions from the MC simulations are shown in Fig. 8.

A comparison of the simulated distributions with those of C_5^-[7] is relevant. The peaks found in these distributions appear because the sparse level density for C_5 at the low energy product states strongly reduces photon emission. They are absent for C_7^- because of the higher level density of the neutral molecule. The nature of the radiative cooling, on the other hand, is vibrational, similar to that of C_5^-.

SUMMARY

The spontaneous and the photo-enhanced decays of C_7^- produced in a laser ablation source have been measured. The spontaneous decay, the laser enhanced yield, and the decay of the enhanced signal were simulated with MC calculations. The simulations with published IR integrated absorption coefficients were able to reproduce all three measured signals with the same radiative cooling, without any correcting factor on the oscillator strengths, as was previously found necessary for similar experiments on C_5^-. The neutralization yields vs. time were found to scale, with a scaling factor that varied with time to the power 0.7. The scaling allowed conversion of the data to energy distributions. The energy distribution is created in the source but is modified by depletion by spontaneous electron emission and later, within a few ms, by radiative cooling. The radiative cooling shapes the energy distribution into an almost Gaussian form with a mean and a width that both decrease with time to the power −0.7. A similar scaling with an identical power was previously found for C_5^- which, like C_7^-, cools predominantly by infrared emission of a single vibrational transition. The generality of the observed scaling and the value of the power −0.7 remains an open question.

ACKNOWLEDGMENTS

This work has been supported by the Department of Physics at the University of Gothenburg, the Swedish Foundation for International Cooperation in Research and Higher Education (STINT), the TMU Research Program Grant 2010-2012 "Electrostatic Ion Storage Ring for Molecular Science," and 2013–2014 "Ion Storage Experiments for Interstellar Chemistry."

[1] A. G. G. M. Tielens, Rev. Mod. Phys. **85**, 1021 (2013).
[2] K. Hansen and E. E. B. Campbell, J. Chem. Phys. **104**, 5012 (1996).
[3] J. U. Andersen, C. Brink, P. Hvelplund, M. O. Larsson, B. B. Nielsen, and H. Shen, Phys. Rev. Lett. **77**, 3991 (1996).
[4] J. U. Andersen, C. Gottrup, K. Hansen, P. Hvelplund, and M. O. Larsson, Eur. Phys. J. D **17**, 189 (2001).
[5] S. Tomita, J. U. Andersen, C. Gottrup, P. Hvelplund, and U. V. Pedersen, Phys. Rev. Lett. **87**, 073401 (2001).
[6] J. U. Andersen and E. Bonderup, Eur. Phys. J. D **11**, 413 (2000).
[7] M. Goto, A. E. K. Sundén, H. Shiromaru, J. Matsumoto, H. Tanuma, T. Azuma, and K. Hansen, J. Chem. Phys. **139**, 054306 (2013).
[8] G. Ito, T. Furukawa, H. Tanuma, J. Matsumoto, H. Shiromaru, T. Majima, M. Goto, T. Azuma, and K. Hansen, "Cooling dynamics of photo-excited C_6^- and C_6H^-" (to be published).
[9] S. Martin, J. Bernard, R. Brédy, B. Concina, C. Joblin, M. Ji, C. Ortega, and L. Chen, Phys. Rev. Lett. **110**, 063003 (2013).
[10] S. Jinno, T. Takao, K. Hanada, M. Goto, K. Okuno, H. Tanuma, T. Azuma, and H. Shiromaru, Nucl. Instrum. Methods Phys. Res. A **572**, 568 (2007).
[11] J. U. Andersen, E. Bonderup, and K. Hansen, J. Phys. B **35**, R1 (2002).
[12] K. Hansen, *Statistical Physics of Nanoparticles in the Gas Phase* (Springer, Netherlands, 2013).
[13] J. Szczepanski, S. Ekern, and M. Vala, J. Phys. Chem. A **101**, 1841 (1997).
[14] J. M. L. Martin, J. El-Yazal, and J.-P. François, Chem. Phys. Lett. **242**, 570 (1995).
[15] D. W. Arnold, S. E. Bradforth, T. N. Kitsopolous, and D. M. Neumark, J. Chem. Phys. **95**, 8753 (1991).
[16] S. Diaz-Tendero, G. Sánchez, P. A. Hervieux, M. Alcamí, and F. Martin, Braz. J. Phys. **36**, 529 (2006).
[17] Y. Tai, J. Maurakami, Y. Maruyama, W. Yamaguchi, T. Mizoya, K. Igarashi, and S. Tanemura, J. Phys. Chem. B **103**, 5500 (1999).
[18] *Handbook of Mathematical Functions*, edited by M. Abramowitz and I. A. Stegun (Dover Publications, New York, 1972).
[19] K. Hansen, J. U. Andersen, P. Hvelplund, S. P. Møller, U. V. Pedersen, and V. V. Petrunin, Phys. Rev. Lett. **87**, 123401 (2001).